

An Integrated Method for Determination of the Oswald Factor in a Multi-Fidelity Design Environment

Daniel Böhnke, Jonas Jepsen, Till Pfeiffer, Björn Nagel, Volker Gollnick

Air Transportation Systems, DLR e.V., Blohmstr. 18, 21079 Hamburg

Carsten Liersch

Institute of Aerodynamics and Flow Technology, DLR e.V., Lilienthalplatz 7, 38108 Braunschweig

Keywords: *Multi-Fidelity, CPACS, Distributed Design Environment*

Abstract

Aircraft conceptual design often focuses on unconventional configurations like for example forward swept wings. Assessing the characteristics of these configurations usually requires the use of physic based analysis modules. This is due to the fact that for unconventional configurations no sufficient database for historic based analysis modules is available.

Nevertheless, physic based models require a lot of input data and their computational cost can be high. Generating input values in a trade study manually is work-intensive and error-prone.

Conceptual design modules can be used to generate sufficient input data for physic based models and their results can be re-integrated into the conceptual design phase. In this study a direct link between a conceptual design module and an aerodynamic design module is presented. Geometric information is generated by the conceptual design module and the physic based results, in form of the Oswald factor, are then fed back.

Apart from the direct link, an equation for determination of the Oswald factor is derived via a Symbolic Regression Approach.

1 Introduction

At early stages of design large parts of the overall costs are fixed, since decisions have a major influence on the global configuration, [1]. It is therefore important to determine the characteristics of an aircraft as early and accurately as possible.

In a simplified treatment, analysis modules can be grouped into historic and physic based models. Historic based models are quick to evaluate due to their statistic approach and deliver reliable results for conventional configurations. The necessary inputs are few. Physic based models are, depending on the level of detail, more cost intensive to evaluate and require more input, e.g. a detailed geometry description. Nevertheless, these modules are more accurate, especially for unconventional configurations.

Hence, at the earliest stages of the design only historic based models can be applied, since the necessary input data for physic based models is not available yet. These models are however unsuitable for most new configurations since they are based on the existing design space, and can not be used for assessment in the diverging phases of design, [2]. At this point in time, unconventional configurations should already be a

part of the design space. In a simplified declaration, historic models are categorized in conceptual design and physic based models in preliminary design.

The question arises whether it is possible to close the gap between conceptual and preliminary design, i.e. historic and physic based analysis. Preferably this should be accomplished in an automated manner, to make the results of physic based analysis available at an earlier point of the design.

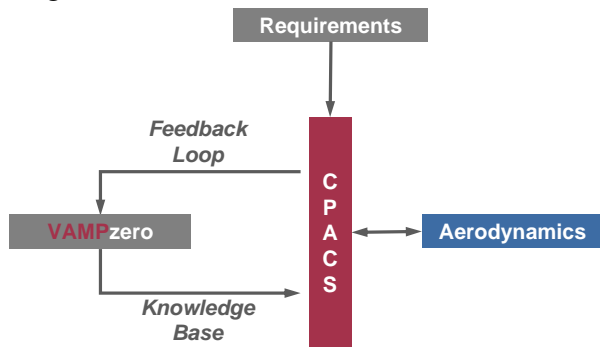


Fig. 1: Multi-Fidelity Process

Within this study a central model approach (CPACS) is proposed that combines a historic based conceptual design module (VAMPzero) with a physic based aerodynamic module (LIFTING_LINE), [3, 4]. As use-case the calculation of the Oswald factor is chosen. On a first step, a set of requirements is defined and fed into the conceptual design tool. With knowledge based engineering techniques a detailed geometry definition is derived from the conceptual design and stored in the central model data format. The aerodynamic module is linked to the central model and triggered without further user input. The resulting aerodynamic performance map is subsequently reduced to the Oswald factor and reused within the conceptual design module. Provided that a sufficient number of trades is carried out, a symbolic regression approach, [5] is applied to derive new conceptual design methods from the multi-fidelity loop, as displayed in Figure 1.

The paper is grouped into six sections: This section gives a short introduction. Section 2 elaborates on existing methods for the determination for the Oswald factor in conceptual design. The proposed design environment is described in Sec-

tion 3. A trade study is then carried out and examined in Section 4. Finally, a discussion of the results is given in Section 5 and some conclusions and an outlook in Section 6.

2 State of the Art

In this section an overview is given for the calculation of the Oswald factor (e) in conceptual and preliminary design. The Oswald factor is needed for the estimation of the lift induced drag (C_{D_i}), whereas drag due to lift (C_{D_L}) in this paper is meant to take into account lift induced drag and drag due to viscous forces (C_{D_v}). The calculation of the wave drag (C_{D_w}) is not considered any further. The lift induced drag in conceptual design is usually noted as in Eq. 1:

$$e = \frac{1}{\pi AR} \frac{C_L^2}{C_{D_i}} \quad (1)$$

Additionally, the drift for the zero lift angle of attack (C_{L_0}) needs to be taken into account. Furthermore, local lift distributions may result in lift induced drag even if the overall lift sums up to zero, e.g. for twist distributions. Therefore a parameter for induced drag at zero lift ($C_{D_{i0}}$) is introduced. Equation 1 is then extended to Eq. 2:

$$e = \frac{1}{\pi AR} \frac{(C_L - C_{L0})^2}{(C_{D_i} - C_{D_{i0}})} \quad (2)$$

The first outlined approach originates from Raymer and is based on the aspect ratio (AR) and the leading edge sweep angle of the wing (Λ), [6]. Two different equations valid for unswept (Eq. 3) and swept (Eq. 4) wings are defined.

$$e = 1.78(1 - 0.045AR^{0.68}) - 0.64 \quad (3)$$

$$e = 4.61(1 - 0.045AR^{0.68})(\cos(\Lambda))^{0.15} - 3.1 \quad (4)$$

with $\Lambda > 30$

These equations can be evaluated quickly as the number of variables is low. Drawbacks exist because the design space is limited to a specific area via the limitations on the leading edge sweep angle.

An approach by Howe (Eq. 5) takes into account additional parameters like the flight Mach

number (M_N), the taper ratio (λ) and the thickness to chord ratio (t/c), [7]. The equations derived by Howe are defined for drag due to lift and it is hard to extract an exact formulation for the Oswald factor. Nevertheless, they are included in this overview to display complex symbolic equations known in conceptual design as we will derive such an equation at a later point of this study. The functions for the taper ratio and aspect ratio are given in Eq. 6 and Eq. 7:

$$C_{Di} = \frac{(1 + 0.12M_N^6)}{\pi AR} \quad (5)$$

$$\left[1 + g(AR) + \frac{0.142 + ARf(\lambda)(10t/c)^{0.33}}{\cos(\Lambda)^2} \right] \quad (6)$$

$$f(\lambda) = 0.005 \left[1 + 1.5(\lambda - 0.6)^2 \right] \quad (6)$$

$$g(AR) = \frac{0.1}{(4 + AR)^{0.8}} \quad (7)$$

A semi physic based approach is described by Jenkinson for the induced drag utilizing lifting-line theory, [8, 9]. The approach leads to a function (C_1) depending on the taper ratio and aspect ratio, as shown in Figure 2.

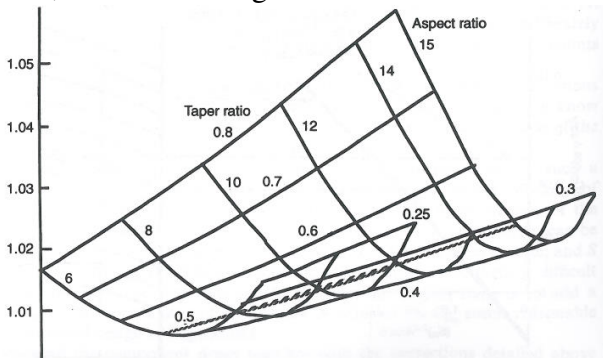


Fig. 2: C_1 depending on λ and AR , from [8]

Subsequently, the results are corrected for conventional (Eq. 8) and CFD (Eq. 9) wing design so that e results in C_2 over C_1 . For the change in drag due to lift due to viscous forces a formulation is used that is based on the zero lift drag.

$$C_2 = 1.235 - 0.0245AR \quad (8)$$

$$C_2 = 1.113 - 0.0116AR \quad (9)$$

The results from Jenkinson already implement a physic based model. In this study this approach

will be extended by a set of relevant variables with their corresponding formulation.

3 Design Environment

In a generalized manner, a distributed design environment consists of three components. The basis for all communication is a *common language* that is achieved via a central model approach. The second component is a set of *analysis modules* that can exchange information using the common language. The benefits of using a central model are depicted in Figure 3. Due to the fact that communication now only exists between the analysis modules and the central model the number of interfaces decreases. Additionally, interaction between the analysis modules is decreased in a way that different modules can be utilized for similar tasks. For example a fuselage weight prediction can be made using a historic based or a physic based, either beam or shell, model. Regardless from the chosen analysis strategy, the fuselage mass is included in the overall design and available for further modules.

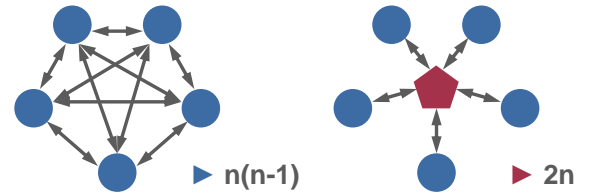


Fig. 3: Central Model Approach

This process of communication is guided by an *engineering framework*. The engineering framework also takes over general tasks like process control and optimization. As can be seen from Figure 1, in the current study the Common Parametric Aircraft Configuration Schema (CPACS) is used as the central model and VAMPzero and LIFTING_LINE as the analysis modules. For the engineering framework the Remote Component Environment (RCE) is used.

3.1 CPACS

Since 2005 CPACS is under development at DLR, [3]. It is a XML-based definition of the air transportation system. Historically, the fo-

cus is set on aircraft nevertheless the bandwidth of applications spreads from conceptual and preliminary aircraft design to climate impact modeling and engine design, [4, 10, 11]. Using a central model enables an easy communication for designers as the underlying model stays the same. Additionally, tool development becomes more efficient as core tasks can be unified. For example CPACS comes with supplementary libraries for geometry handling and visualization as well as CPACS specific XML functionalities. Furthermore, XML toolboxes are available for most programming languages both commercial and open source. One important feature of CPACS is the handling of product and process information, i. e. not only the aircraft is described but also *tool-specific* information to control parts of the analysis process, e. g. the number of panels on a wing for aerodynamic analysis.

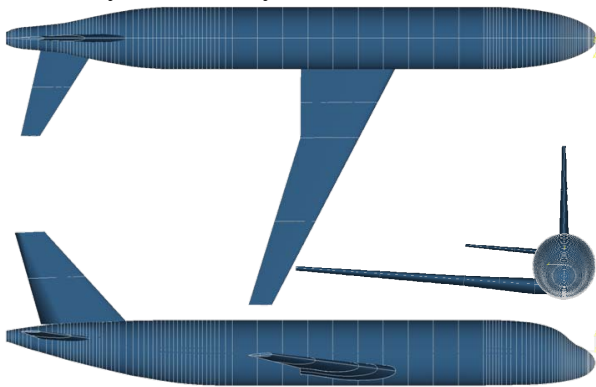


Fig. 4: Baseline Geometry

In Figure 4 a sample geometry in CPACS is displayed. This geometry is generated by VAMPzero (s. Section 3.3) and is the baseline for the trade study (s. Section 4). It shows a conventional short range configuration in a quasi-symmetrical view.

3.2 LIFTING_LINE

In the aerodynamic analysis the CPACS dataset is imported via an interface tool to trigger the multiple lifting line program LIFTING_LINE, [9]. The interface from LIFTING_LINE to CPACS and the interaction with other analysis modules is outlined in more detail by Liersch et. al. in [3]

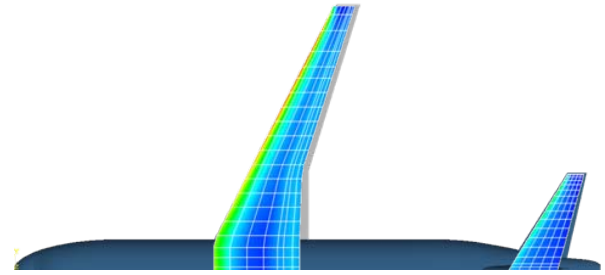


Fig. 5: Lift Distribution for Baseline Aircraft

LIFTING_LINE enables a calculation of the lift induced drag from which the Oswald factor is derived. A lift distribution for the baseline geometry is depicted in Figure 5.

Additionally, the outlined research benefits from the low computing cost of a single computation. Calculation times from LIFTING_LINE are in the order of few seconds and only minor overhead occurs due to file transfer and model transformation.

3.3 VAMPzero

For the purposes of DLR's distributed multidisciplinary design environment a new conceptual design module is developed. VAMPzero is based on handbook methods taken from well-known design literature, [6, 7, 12]. The key modeling aspects of VAMPzero are described in more detail in [4].

In a design environment that is mostly based on preliminary level, two possible tasks remain for a conceptual design tool. The first one is the initialization of the datasets. Designers usually need to start working with only the top level aircraft requirements (TLAR) at hand. In this case the conceptual design code can close the gap between the TLAR and sufficient information to trigger preliminary analysis modules.

To overcome the gap, the results from the conceptual design are transferred into CPACS via a knowledge based engineering approach. For the conceptual design calculations and sizing VAMPzero uses a single trapez wing shape. For the export the wing shape can be mapped to a double trapez with an additional rectangular section up to the wing-fuselage intersection. Figure 6 shows the geometry. The wing planform is described by the wing span (b_w), the leading

edge sweep, the aspect ratio, the taper ratio, and the kink ratio (η_k). The trailing edge from root to kink is perpendicular to the fuselage. The twist angle (ϑ) is applied in a linear distribution from root to tip. Thickness to chord ratios at root and tip stations are a result from VAMPzero. For the empennage symmetrical airfoils are used. The wing geometry is generated with NACA-6 series airfoil. Further airfoil sets and their assortment is an ongoing topic within the development of VAMPzero.

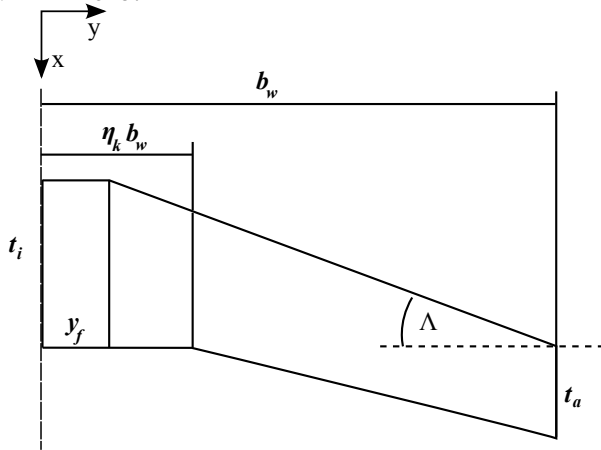


Fig. 6: Double Trapezoid Wing

Using the Π -Theorem by Buckingham dimensionless parameters for the description of the geometry can be defined as in Table 1 to describe the introduced wing geometry [13, 14]. During the mapping to CPACS Π_1 to Π_4 are constant to assure geometric similarity to the single trapez wing. Π_5 and Π_6 are then derived for a constant wing reference area ($S_{ref} = f(t_i, t_a, b_w, \eta_f, \eta_k, \varphi)$) and the fuselage diameter.

Table 1: Dimensionless Constants

$\Pi_1 = \Lambda$	$\Pi_2 = \vartheta$	$\Pi_3 = \lambda = \frac{t_a}{t_i}$
$\Pi_4 = AR = \frac{4b_w^2}{S_{ref}}$	$\Pi_5 = \eta_k = \frac{y_k}{b_w}$	$\Pi_6 = \eta_f = \frac{y_f}{b_w}$

The fuselage shape is derived from a baseline configuration that is afterwards scaled to fit to the results from the conceptual design. The empennage is exported *as is* as single trapez surfaces. In this way the conceptual design tool can generate geometries as shown in Figure 4 and all additional data to trigger a LIFTING_LINE analysis.

The second task for a conceptual design tool in a preliminary design environment is the integration of results. Results from several higher level analysis modules need to be aggregated to obtain the effects on the overall aircraft configuration. For example, the wing mass in the mass breakdown is overwritten by higher level analysis module (e.g. FEM) and VAMPzero takes these changes into account when re-calculating the aircraft. In the case of this study, VAMPzero interprets the results from LIFTING_LINE to derive the Oswald factor and calculate a new configuration.

3.4 RCE

VAMPzero and LIFTING_LINE exchange information via CPACS. To establish this connection also in a distributed environment where parallelization, optimization and design of experiments are possible an engineering framework is needed. RCE is a general engineering framework that is specialized for this task via the Chameleon tool suite, [15, 16]. Chameleon originates from the beginnings of CPACS development within the Technology Integration for the Virtual Aircraft (TIVA) project and is now integrated into RCE.

RCE offers a graphical user interface to connect analysis modules and run different stages of the design process. As a first step a workflow is set up and is sent to executing computers. All information created during the analysis, e.g. intermediate results, tool-specific outputs, transferred datasets, is available via an integrated data management system.

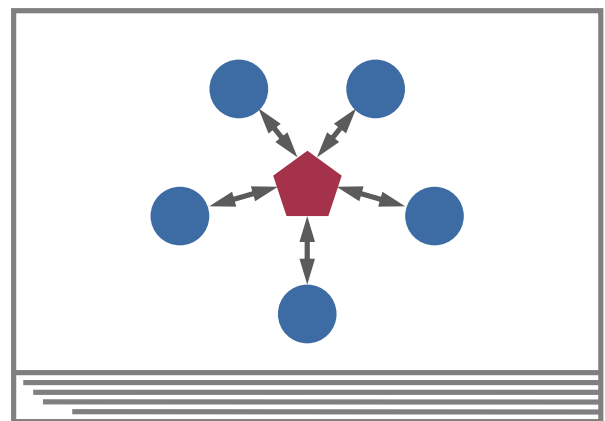


Fig. 7: Distributed Design Environment

The integrated Chameleon tool suite enables disciplinary experts to wrap their tools in the distributed design environment. Global operations like file transfer, remote execution and XML-mappings, as well as local operations like the interpretation of CPACS files are supported by Chameleon. Additionally, a geometric library offers CPACS-specific operations to extract information from datasets.

3.5 Eureqa

The goal of this study is to derive a method for determination of the Oswald factor that is both accurate and available at low computational cost. Symbolic regression is a suitable tool to find equations from experimental data, [5].

The input for Eureqa, the symbolic regression toolbox used in this study, consists of a set of input variables along with the corresponding experimental results. Additionally, mathematical operators are specified that shall be used in the equation. Several combinations of operators and variables are then generated by a genetic algorithm to find a suitable approximation in form of a symbolic equation. Derived equations are rated for their complexity and fit.

In the current study Eureqa is used as a post processor. Future research might include it in the calculation loop. In this way Eureqa can define new design points where the current solution does not fit to the design space. Therefore the number of necessary runs could be decreased.

4 Trade Study

The baseline configuration for this study is a single aisle ($nPAX = 150$), medium range ($R = 3000km$, $Mach = 0.78$) aircraft.

To determine the effects of different parameters on the lift induced drag, design variables are varied as shown in Table 2. Due to the fact that the number of dimensions and the range of the variables are large, a full factorial design is unsuitable. Instead the design space is explored by Latin-Hypercube sampling. Apart from the specified values for the baseline configuration the reference area for the wing is kept constant.

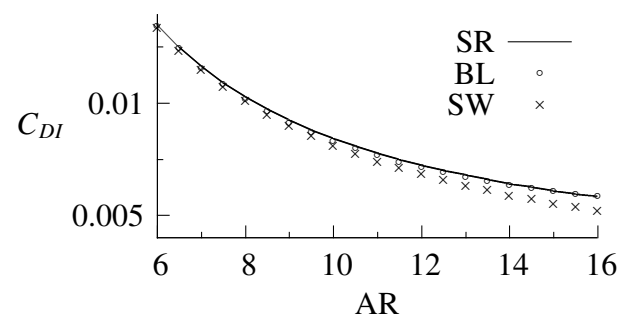
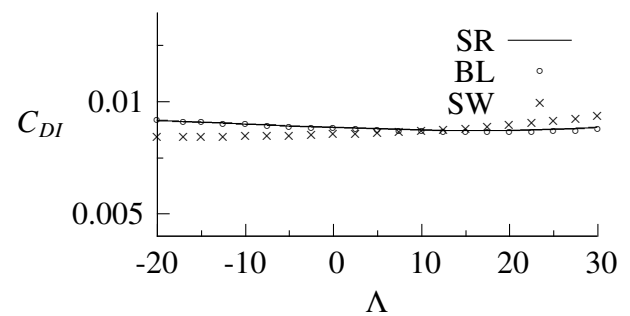
Table 2: Design Space

Variable	Symbol	Range
Sweep Angle	Λ	-20.0 - 30.0
Aspect Ratio	AR	6.0 - 16.0
Taper Ratio	λ	0.1 - 0.6
Twist Angle	ϑ	-10.0 - 0.0
Kink Ratio	η_k	0.2 - 0.4

In a distributed design environment one has to cope with the drawbacks of data transfer and interpretation. This leads to some overhead in the calculation time. Nevertheless, more time is spent on the symbolic regression and post processing as the runtimes of VAMPzero and LIFTING_LINE are low.

The trade study is grouped into two parts. In the first part design variables are varied independently from each other. These calculations are used as control data and the analysis of the effects from the different input variables benefits from the transparency of this setup.

The second part of the study consists of a Latin Hypercube sampling in the complete design space. Subsequently, a symbolic regression approach is applied to the results to derive an equation for determination of the Oswald factor. The results of the symbolic regression are then compared to the control data.



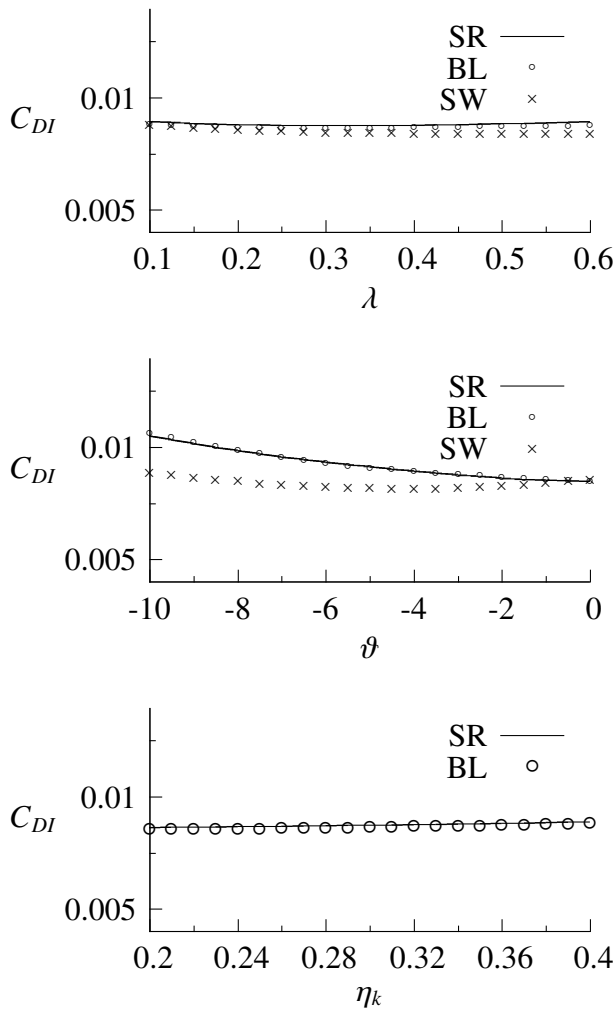


Fig. 8: Trade Study Results

In the first part the baseline parameters ($\Lambda = 28$, $AR = 9.5$, $\lambda = 0.2$, $\vartheta = -2$, $\eta_k = 0.35$) are kept constant and only one design variable is varied. The results are displayed as baseline (BL) in Figure 8. Additionally, a set of the trades was carried out with a single trapez geometry. The parameters are varied in the same design space but the wing is unswept and untapered, i.e. $\Lambda = 0$, $AR = 9.5$, $\lambda = 1$, $\vartheta = 0$. For the single trapez the kink parameter is ignored. The results are marked as (SW) in Figure 8. All plots are made on the same scale to illustrate the impact on the lift induced drag in comparison. Displayed values are shown for a constant lift coefficient ($C_L = 0.5$). These parts of the trade study serve as the control data for the derived equation from the Latin-Hypercube sampling.

The second part consists of the previously named Latin-Hypercube sampling. A number

of 500 samples throughout the complete design space is calculated. The data from this sampling is fed into a symbolic regression toolbox to derive a symbolic formulation for the lift induced drag in dependence on the design variables.

For comparison of the method these simplified graphs are shown as SR in Figure 8. The symbolic formulations are noted in Eq. 10. The solution derived from the Latin-Hypercube sampling is valid in the full range of the design space.

5 Discussion

This chapter contains a discussion of the results found from Figure 8 as well as more general review of the introduced design environment and calculation strategy.

For the wing sweep the minimum for the lift induced drag for the single trapez is at a forward swept position. The double trapez minimum lies at approximately $\Lambda = 23$. The difference in the results can be explained by the additional taper for the double trapez wing that already shifts the load distribution in spanwise direction.

The results for the aspect ratio both for the single and the double trapez wing show similar trends. As the results are plotted for the lift induced drag the influence of the aspect ratio is increased, see Eq. 1, where the Oswald factor is now also a function of the aspect ratio. At medium aspect ratios the derived equation overpredicts the lift induced drag.

Curves for the taper ratio align at smaller taper ratios. For the unswept wing the minimum lift induced drag is located at taper ratios larger than the considered design space. The minimum for the unswept single trapez lies within the design space but sensitivity is low compared to the aspect ratio. For larger taper ratios the derived equation produces higher values of lift induced drag.

Twist is applied linear on both wings. For the double trapez there are three twisted sections: fuselage section, kink section and tip section. The single trapez wing is only twisted at the tip. For the double trapez the lift induced drag can not be decreased by additional twist. A coupling with a structural tool would give more de-

$$e = 0.04 - 0.0007AR - 0.00019\Lambda\theta + \lambda^{0.03} \cos(0.16 - 0.0007ARA - 0.0007AR\Lambda\eta - 0.55\lambda) \quad (10)$$

tails on the benefits from twist due to load reduction at the tip. The single trapez wing can still benefit from the twist. The fitted curve is in accordance with the baseline. The twist has a high influence on $C_{D_{10}}$. The aerodynamic (in)efficiency can therefore not be described by the Oswald factor alone.

As already mentioned, the change in the kink ratio only applies to the double trapez wing. The more the kink moves outward the higher the lift induced drag. This is due to the fact that the inward area increases rapidly in comparison the outer part of the wing. The symbolic regression constantly over estimates the lift induced drag.

The plots show a good agreement between the derived equations and the single parameter variations. The root mean squared error for the Oswald factor is 0.011. This gives confidence to implement the derived equation (Eq. 10) into the conceptual design tool VAMPzero. As all parameters that are needed to generate the higher level geometry are available in VAMPzero no additional customizations of the code are necessary.

The outlined study focuses on the interaction of analysis modules on different levels of fidelity. As it was desired to derive a new calculation method in a large design space the number of design evaluations was high. In this case the study benefitted from the fact that LIFTING_LINE offers a physic based approach at low computational cost. It is questionable at which cost a similar approach is possible with higher detail models, e.g. CFD.

Integration of higher level analysis modules often is done using response surface models. In this way the computational time is kept low, as most of it is spent a-priori. Within the outlined method this approach is possible as seen from the derived equation. Additionally, the direct link between VAMPzero and the disciplinary analysis module LIFTING_LINE is existent and needs to be triggered as soon as the design space is enlarged

It is shown that the derived equation from the symbolic regression approach fits well to the con-

trol data. It is assumed that reliable results can be obtained within the area of the design space. A detailed assumption on the validity of the equation outside of the design space is not yet given.

Finally, it is possible to automatize large parts of the analysis chain. Nevertheless the extraction of knowledge is not yet possible in a similar way. This is due to practical reasons, as the process works also well regardless of faulty data. For validation and verification the *Engineer in the Loop* is a necessity.

6 Conclusion

The current study outlines a methodology to derive the Oswald factor in a multi-fidelity environment. This methodology can be extended for different use cases targeting single higher fidelity analysis modules, e.g. for mass estimation. For future research the target is to analyze couplings of higher fidelity tools, as for example in aeroelastics, and try to reflect these couplings also on the level of a simple analysis module such as VAMPzero. These couplings are not necessarily limited to different disciplines but may also couple analysis modules of different fidelity levels.

Within the outlined approach the *curse of dimensionality* is of crucial importance, [17]. Due to the fact that the number of design variables is usually beyond two, the number of calculation runs increases rapidly. Determining the number of required runs for a good fit is currently only a smart guess. Integrating the symbolic regression toolbox into the design loop may give the chance to optimize this process. The symbolic regression algorithm is capable of deriving new experiments at locations in the design space where the current error is high. Starting from a small number of calculation, e.g. a full factorial design only on the outer limits of the design space, the design loop could be configured until the overall error reaches a certain minimum.

Acknowledgements

The authors would like to thank Markus Litz, Markus Kunde, Arne Bachmann and Doreen Seider from DLR Simulation and Software Technology for their support on the engineering framework and Chameleon. Additionally, the authors would like to thank Markus Schmidt and Hod Lipson from Cornell University for making the Eureqa toolbox available.

References

- [1] Stark, J., "Product Lifecycle Management , 21st Century Paradigm for Product Realisation," *Springer London*, 2005.
- [2] La Rocca, G. and van Tooren, M., "Enabling distributed multi-disciplinary design of Complex Products : a knowledge based Engineering Approach," *Journal of Design Research*, Vol. 5, 2007, pp. 333–352.
- [3] Liersch, C. and Hepperle, M., "A Unified Approach for Multidisciplinary Aircraft Design," *CEAS European Air and Space Conference*, 2009.
- [4] Böhnke, D., Nagel, B., and Gollnick, V., "An Approach to Multi-Fidelity in Conceptual Aircraft Design in Distributed Design Environments," *IEEE Aerospace Conference*, 2011.
- [5] Schmidt, M. and Lipson, H., "Distilling Free-Form Natural Laws from Experimental Data," *Science*, Vol. 324, 2009, pp. 81–85.
- [6] Raymer, D., "Aircraft Design: A Conceptual Approach," *AIAA Education Series*, 1989.
- [7] Howe, D., "Aircraft Conceptual Design Synthesis," *Professional Engineering Publishing*, 2000.
- [8] Jenkinson, L., Simkin, P., and Rhodes, D., "Civil Jet Aircraft Design," *Butterworth Heinemann*, 1999.
- [9] Horstmann, K. H., "Ein Mehrfach-Traglinienverfahren und seine Verwendung für Entwurf und Nachrechnung nicht-planarer Flügelanordnungen," *DFVLR-FB 87-51*, 1981.
- [10] Zill, T., Böhnke, D., Nagel, B., and Gollnick, V., "Preliminary Aircraft Design in a Collaborative Multidisciplinary Design Environment," *AIAA Aviation Technology, Integration and Operations Conference*, 2011.
- [11] Koch, A., Lührs, B., Dahlmann, K., Linke, F., Grewe, V., Plohr, M., Nagel, B., Gollnick, V., and Schumann, U., "Climate impact assessment of varying cruise flight altitudes applying the CATS simulation approach ," *CEAS European Air and Space Conference*, 2011.
- [12] Roskam, J., "Airplane Design," *DARCorporation*, Vol. I-VII, 1989.
- [13] Buckingham, E., "On Physically Similar Systems; Illustrations of the Use of Dimensional Equations," *Physical Review*, 1914, pp. 345–376.
- [14] Jepsen, J., "Wissensbasierte Erstellung von Geometrien auf der Grundlage von Handbuchverfahren," *IB-328-2011-07, TU Hamburg-Harburg*, 2011.
- [15] Litz, M., Bachmann, A., and Kunde, M., "TIVA XML Interface," *tixi.googlecode.com*.
- [16] Litz, M., Bachmann, A., and Kunde, M., "TIVA Geometric Library," *tigl.googlecode.com*.
- [17] Koch, P. N., Simpson, T., Allen, J. K., and Mistree, F., "Statistical Approximations for Multidisciplinary Design Optimization: The Problem of Size," *Journal of Aircraft*, Vol. 36, 1999, pp. 275–286.